Title

HLA-DR-expressing fibroblast-like synoviocytes are inducible antigen presenting cells that present autoantigens in Lyme arthritis

Authors

Joseph R Rouse[1], Rebecca Danner[1], Amanda Wahhab[1], Michaela Pereckas[2], Mecaila E McClune[3,4], Allen C Steere[5], Klemen Strle[6], Brandon L Jutras[3,4], Robert B Lochhead[1,7]

Affiliations

[1] Department of Microbiology and Immunology, Medical College of Wisconsin, Milwaukee, WI, USA

[2] Department of Biochemistry, Medical College of Wisconsin, Milwaukee, WI, USA

[3] Department of Biochemistry, Virginia Tech, Blacksburg, VA, USA

[4] Center for Emerging, Zoonotic and Arthropod-borne Pathogens, Virginia Tech, Blacksburg, VA, USA

[5] Center for Immunology and Inflammatory Diseases, Division of Rheumatology, Allergy, and Immunology, Massachusetts General Hospital, Harvard Medical School, Boston, MA, USA

[6] Department of Molecular Biology and Microbiology, Tufts University School of Medicine, Boston, MA, USA

[7] Division of Rheumatology, Department of Medicine, Medical College of Wisconsin, Milwaukee, WI, USA

Send correspondence to: Robert B Lochhead, PhD, Medical College of Wisconsin Department of Microbiology and Immunology BSB-2850, 8701 Watertown Plank Road, Milwaukee, Wisconsin, 53226, USA

Email address: rlochhead@mcw.edu

Telephone number: 414-955-4882

AUTHORS' SUMMARY

This study demonstrates that IFNγ-activated MHC-II+ fibroblast-like synoviocytes (FLS) stimulated with *Borrelia burgdorferi* present foreign and self MHC-II antigens, including Lyme autoantigens. Furthermore, IFNγ-activated MHC-II+ FLS stimulated with *B. burgdorferi* peptidoglycan can induce activation and proliferation of naïve CD4+ T cells in an MHC-II antigen-dependent manner, demonstrating that activated MHC-II+ FLS are inducible antigen presenting cells.

ABSTRACT

Background: HLA-DR-expressing fibroblast-like synoviocytes (FLS) are a prominent cell type in synovial tissue in chronic inflammatory forms of arthritis. We recently showed that peptides from several extracellular matrix (ECM) proteins, including fibronectin (FN1), were immunogenic CD4+ T cell epitopes in patients with postinfectious Lyme arthritis (LA). However, the role of FLS in presentation of these T cell epitopes remains uncertain.

Methods: Primary LA FLS and primary murine FLS stimulated with interferon gamma (IFNγ), *Borrelia burgdorferi*, and/or *B. burgdorferi* peptidoglycan (PG) were assessed for properties associated with antigen presentation. HLA-DR-presented peptides from stimulated LA FLS were identified by immunopeptidomics analysis. OT-II T cells were cocultured with stimulated murine FLS in the presence of OT-II antigen to determine the potential of FLS to act as inducible antigen presenting cells (APC).

Results: FLS expressed HLA-DR molecules within inflamed synovial tissue and tendons from patients with post-infectious LA patients *in situ.* MHC class II and costimulatory molecules were

expressed by FLS following *in vitro* stimulation with IFNγ and *B. burgdorferi* and presented both foreign and self MHC-II peptides, including T cell epitopes derived from two Lyme autoantigens fibronectin (FN1) and endothelial cell growth factor (ECGF). Stimulated murine FLS induced proliferation of naïve OT-II CD4+ T cells, particularly when FLS were stimulated with both IFNγ and PG.

Conclusions: MHC-II+ FLS are inducible APCs that can induce CD4+ T cell activation and can present Lyme autoantigens derived from ECM proteins, thereby amplifying tissue-localized autoimmune CD4+ T cell responses in LA.

INTRODUCTION

Human leukocyte antigen DR-expressing fibroblast-like synoviocytes (HLA-DR+ FLS) are believed to be key drivers of synovial inflammation (1-5). We have recently demonstrated that synovial extracellular matrix (ECM) proteins, including fibronectin (FN1), are targets of autoimmune CD4+ T cell responses in over half of patients with postinfectious Lyme arthritis (LA), defined as patients who fail to fully resolve their arthritis after 2-3 months of appropriate antibiotic therapy and apparent killing of the Lyme disease spirochete *Borrelia burgdorferi*. FLS are major producers of ECM proteins, and HLA-DR+ FLS are highly abundant in postinfectious LA synovial tissue (6), and we have hypothesized that FLS are both producing and presenting Lyme autoantigens (1, 2). However, this hypothesis has not yet been fully tested.

FLS are synovial tissue resident cells that are important in joint health and disease. FLS are 1) the primary cell type within joint synovial tissue; 2) responsible for production and maintenance of extracellular matrix; 3) critical for tissue repair; and 4) required to achieve homeostasis following an inflammatory insult (7). Under chronic inflammatory conditions, however, FLS play a critical role in driving pathogenesis. In RA, the prototypic autoimmune joint disease, activated HLA-DR+ FLS accumulate within the synovial lining and sub-lining, where

they interact with CD4+ T cells and other immune cells (8-13). Furthermore, abundance of activated HLA-DR+ FLS positively correlates with RA disease activity (14).

Lyme disease (LD) is caused by the tick-borne spirochete *Borrelia burgdorferi* and occurs primarily in temperate zones of North America, Europe, and Asia. Each year, an estimated 500,000 new cases occur in the U.S. and the infection is endemic in certain locations in northeastern states (15, 16). LA is the most common late-stage LD manifestation in the U.S. and is usually effectively treated with 1-3 months of oral and/or IV antibiotic therapy, called antibiotic-responsive LA (17). However, in a subset (~10%) of patients, arthritis can persist or worsen, even after apparent spirochetal killing by appropriate antibiotic therapy, called post-infectious LA (17). Post-infectious LA is characterized by severe synovial hyperplasia and accumulation of large numbers of HLA-DR+ FLS within inflamed joints (2, 6, 18-20), and is frequently accompanied by autoimmune T and B cell responses targeting self-proteins associated with vascular inflammation and ECM damage (1, 2, 17, 21-24). In addition, peptidoglycan (PG), a pathogen-associated molecular pattern (PAMP) that is an essential cell wall component in most bacteria required for protection from osmotic pressure, is a key *B. burgdorferi* antigen that can persist in joints of post-infectious LA patients up to several years following oral and/or IV antibiotic therapy. This spirochetal remnant may contribute to persistent arthritis after the infection itself is cleared (25, 26).

Bacterial PG has also been detected in the inflamed synovium of patients with RA (27) and osteoarthritis (OA) (28), suggesting that PG accumulates in synovial tissue, particularly within the context of joint inflammation following an infection, such as in postinfectious LA. Moreover, PG has been reported to have an immune adjuvant effect on FLS (29, 30). In this study, we demonstrate that HLA-DR+ FLS can present MHC class II (MHC-II) epitopes, including a Lyme autoantigen derived from ECM protein FN1, and that primary murine FLS stimulated with IFNγ and *B. burgdorferi* PG can induce proliferation and activation of CD4+ T cells in an antigen-dependent manner.

RESULTS

Human LA FLS express HLA-DR within synovial tissue and inflamed tendons

Synovial hyperplasia and accumulation of activated FLS expressing HLA-DR MHC-II molecules are hallmarks of human post-infectious LA (2, 6). We examined HLA-DR expression of vimentin+ stromal cells in synovial tissue and tendon biopsies from patients with post-infectious LA (Figure 1A). HLA-DR+/Vimentin+ double-positive stromal cells (e.g., HLA-DR+ FLS) were primarily localized within the synovial sub-lining (Figure 1A, patients 1 & 2), consistent with a similar study examining a larger number of synovial tissue biopsies (6). In two post-infectious LA patients with tenosynovitis for which tendons were available, double-positive cells were also observed primarily along the lining of inflamed joint tendons (Figure 1A, patients 3 & 4). This would mark the first report, to our knowledge, of HLA-DR+ stromal cells observed in post-infectious LA patient tendons, which is consistent with reports of ligamentous tissue as a reservoir of *B. burgdorferi* during chronic Lyme borreliosis (31) and significant tendinopathy seen in LA during active infection (32) and in post-infectious LA (33).

Human LA FLS express genes associated with antigen presentation when stimulated with IFNγ

FLS do not express the canonical B7 costimulatory molecules B7-1 (CD80) or B7-2 (CD86), although FLS express other B7-family costimulatory molecules that may play a role in antigen presentation (34). We examined expression of potential co-stimulatory molecules using a human LA FLS RNAseq dataset generated as part of an earlier study (6). Primary LA FLS were stimulated with either *B. burgdorferi,* IFNγ, or *B. burgdorferi* + IFNγ together, and expression of genes associated with antigen processing and presentation was assessed (Figure 1B). As expected, expression of co-stimulatory molecules B7-1 and B7-2 were not consistently

expressed at levels above zero (Figure 1B). However, other Signal 2 molecules were expressed by FLS. PD-L1 and CD40 were both strongly upregulated in response to IFNγ stimulation, expression of ICOS-LG trended up in response to *B. burgdorferi* + IFNγ stimulation, and expression of B7-H3 trended down with *B. burgdorferi* + IFNγ stimulation (Figure 1B). Expression of genes associated with regulation of the MHC-II locus (e.g., CIITA), Class II antigen loading (e.g., CD74/invariant chain, HLA-DM, and HLA-DO) and presentation to CD4+ T cells (e.g., HLA-DR) was increased in FLS stimulated with IFNγ or IFNγ + *B. burgdorferi*.

Human LA FLS present MHC-II peptides derived from Lyme autoantigens

Post-infectious LA is frequently accompanied by autoimmune T and B cell reactivity against certain HLA-DR-presented self-antigens, which were previously identified in patients' synovial tissue and/or synovial fluid mononuclear cells (SFMCs) using an unbiased immunopeptidomics approach (35). A subset of these Lyme autoantigens is derived from extracellular matrix (ECM) proteins, which include fibronectin 1 (FN1), laminin B2, collagen Vα1, and matrix metalloprotease 10 (1, 22). Another subset is derived from proteins involved in vascular damage, including and ECGF (23), annexin A2 (24), and apolipoprotein B-100 (21). We and others have previously speculated that HLA-DR+ FLS may present some of these autoantigens within inflamed synovial tissue, thereby contributing to tissue-localized CD4+ T cell autoimmunity (1, 2, 6). Furthermore, we presume that autoimmunity is initiated during infection with *B. burgdorferi*.

We used an *in vitro* immunopeptidomics approach using primary human LA FLS to test whether activated HLA-DR+ FLS were able to present MHC-II antigens, including potential Lyme autoantigens and foreign antigens derived from *B. burgdorferi*. FLS were isolated from synovial tissue collected from an LA patient during the post-infectious period (same patient as patient 1 shown in Figure 1A), whose HLA-DRB type is HLA-DRB1*0701/DRB1*1454. Cells

were passaged over six times prior to use to remove any potential antigens retained from the time of initial sample collection. FLS were stimulated with IFNγ and *B. burgdorferi* (strain B31, 10:1 MOI) for 48 hours, following which peptide-HLA-DR complexes were isolated from lysed cells by immunoaffinity capture. HLA-DR peptides were purified by sequential acid elution, as described (35). We used combined liquid chromatography and tandem mass spectrometry analysis (LC-MS/MS) to identify eluted HLA-DR peptides (Figure 2A).

Fixed Value (FV) validator analysis, with a minimum cross-correlation score (Xcorr) of 2.5, was used to identify 695 total peptides (Supplemental Table S1), including 10 peptides derived from *B. burgdorferi* proteins (Supplemental table S2). Of the *B. burgdorferi* proteins, four are predicted to be localized to the inner membrane, three are cytosolic, and two with unknown localization or function. One protein, high temperature requirement family serine protease (HtrA), occurs in both soluble (periplasmic) and membrane-bound forms and is a B cell immunogen in late-stage LD patients (36). Three source proteins were involved in chemotaxis/motility, three in sugar transport, two in transcription and translation. Surprisingly, none of these *B. burgdorferi* peptides were derived from surface lipoproteins, which are immunodominant B cell antigens (37). We identified three low-confidence peptide-spectrum matches (PSM) with potential matches to a peptide from one outer membrane surface lipoprotein MlpD, but none of the three spectra met the 2.5 Xcorr cutoff, therefore it was not included in our table of predicted peptides.

We also identified 685 peptides derived from 367 unique human proteins using FV validation analysis (Supplemental Table S1). The most abundant source protein of peptides identified was the Invariant chain, suggesting FLS are engaging in endogenous formation and transport of MHC class II peptide complexes, and is consistent with CD74 gene expression data from Figure 1B. Proteins associated with the ECM were also abundantly represented in our dataset, with the top three KEGG Pathway functional annotation terms being 1) focal adhesion; 2) alanine, aspartate, and glutamate metabolism; and 3) ECM-receptor interactions.

Interestingly, the peptide size had a binomial distribution, with 433 (63%) of the peptides greater than 25 amino acids long (median length=42), and 262 (38%) of the peptides 9-25 amino acids long (median value=17), the latter being typical of fully processed MHC-II-bound peptides (38).

A second, more stringent Target Decoy (TD) validation analysis was also performed, using both a 1% false discovery cutoff rate and an Xcorr cutoff of 2.5 to minimize the potential number of false positive peptide-spectrum matches. Using this highly stringent method, we identified 73 unique predicted peptides derived from 50 human proteins (Supplemental Table S1), nearly all of which were 13-18 amino acids long, typical of fully processed MHC-II peptides (Figure 2B). Although all 73 peptides were also identified using FV analysis, no *B. burgdorferi*-derived peptides were identified using this stringent TD analysis method. Of the 73 human peptides identified, 14 peptides were predicted to bind to the peptide binding groove of DRB1*0701, and 46 peptides were predicted to bind to the peptide binding groove of DRB1*1454 (Figure 2B), matching the HLA-DRB type of LA Patient 1. WIKI Pathway, KEGG Pathway, and Gene Ontology cellular localization analyses were used to further characterize source proteins of identified HLA-DR peptides (Figure 2C). Peptides from our TD dataset were enriched for proteins involved in ECM interactions, including focal adhesion, ECM-receptor interactions, TGF-beta receptor signaling, and CCL18 signaling, which is induced by collagen and fibronectin produced by FLS (39). Furthermore, source proteins included 4 ECM, 11 secreted, 16 membrane-associated, and 21 cytosolic proteins (Figure 2C).

Among the self-peptides identified by both FV and TD analysis were two derived from LA autoantigens fibronectin (FN1) and endothelial cell growth factor (ECGF) (Table 1). The FN1 peptide we identified, $FN1_{1996\text{-}2010}$, is predicted to bind to *0701; and the ECGF peptide, $ECGF_{457\text{-}467}$, is predicted to bind to *1454. Interestingly, both the $FN1_{1996\text{-}2010}$ and the $ECGF_{457\text{-}467}$ epitopes from our screen are identical or nearly identical to HLA-DR-bound peptides previously isolated from post-infectious LA synovial tissue (35), and match several epitopes from the Immune Epitope Database (IEDB). Notably, the $FN1_{1996\text{-}2010}$ peptide we identified is nearly

identical to an autoreactive CD4+ T cell epitope in a subset of patients with post-infectious LA (1), demonstrating that FLS are able to present Lyme autoantigens.

Table 1. HLA-DR presented peptides derived from LA autoantigens isolated from LA FLS. Superscripts indicate position of the peptide in the parent protein sequence. Underlined amino acids indicate the sequence corresponding to the HLA-DR binding groove. Bold numbers indicate predicted HLA-DR binding alleles corresponding to the HLA type of LA patient 1. IEDB (Immune Epitope Database) epitope ID numbers were retrieved from iedb.org. Abbreviations: FN1 (fibronectin 1), ECGF (endothelial cell growth factor, also called TYMP, thymidine phosphorylase).

Protein	Sequence	Source	Predicted HLA-DR binding (NetMHCIIpan4.0)
FN1	^{1996}APSNLRFLATTPNSL^{2010}	This study	HLA-DRB1*0101, *0102, *0103, *0401, *0403, *0404, *0405, *0408, ***0701***, *0803, *0901, *1001, *1601, DRB3*0202
FN1	^{1996}APSNLRFLATTPNSL^{2010}	Wang et al. 2017	
FN1	^{1996}APSNLRFLATTPNSLLVSW^{2014}	Kanjana et al. 2023	
FN1	^{1996}APSNLRFLATTPNSL^{2010}	IEDB (ID 144206)	
ECGF	^{457}EALVLSDRAPF^{467}	This study	HLA-DRB1*0301, *0305, *1104, *1301, *1302, *1303, *1401, *1402, ***1454***
ECGF	^{462}SDRAPFAAPSPFAE^{475}	Wang et al. 2017	
ECGF	^{455}LQEALVLSDRAPF^{467}	IEDB (ID 1253447)	
ECGF	^{458}ALVLSDRAPFAAPSPFAE^{467}	IEDB (ID 758118)	

IFNγ induces MHC-II expression in murine FLS

In murine LA, FLS are major sources of arthritogenic cytokines and chemokines in *B. burgdorferi*-infected joints (40, 41). Furthermore, *B. burgdorferi* PG, which persists in joints of LA patients for months to several years following antibiotic therapy, is arthritogenic in mice (26). We hypothesized that in post-infectious LA, IFNγ produced by dysregulated T cells and persistent *B. burgdorferi* PG may be inducing FLS into an antigen presenting cell phenotype, driving CD4+ T cell activation in synovial tissue even after the infection itself is resolved using antibiotic therapy (2).

We employed a primary mouse cell culture model of Lyme arthritis to test this hypothesis. First, we used flow cytometric analysis to measure surface expression of H2-Ab1 (I-ab) by stimulated FLS, the MHC-II allele carried by C57BL/6 mice. Primary murine FLS isolated from ankle joints (passage 4) or undifferentiated (M0) bone marrow-derived macrophages (BMDM) from C57BL/6 mice ($1x10^5$ cells/ well) were stimulated *in vitro* with IFNγ (20 ng/mL), purified *B. burgdorferi* PG (10 µg/mL), or both IFNγ+PG. Cells were stimulated for 18 or 72 hours to determine responses to short-term and long-term exposure, respectively. Consistent with similar studies using primary human LA FLS (6), stimulation of C57BL/6 FLS with IFNγ induced upregulation of MHC-II I-ab ~1.5-fold after short-term stimulation, and ~2-fold after long-term stimulation with IFNγ. Long-term stimulation with both IFNγ and *B. burgdorferi* PG induced upregulation of I-ab ~2.5-fold (Figure 3A). MHC-II I-ab expression in IFNγ-stimulated BMDM was also significantly increased ~5-fold at 72 hours post-stimulation, but PG did not affect I-ab expression (Figure 3A). Expression of FLS activation marker Intercellular Adhesion Molecule 1 (ICAM-1), which is important for T cell attachment to APCs during antigen presentation and formation of immune synapses, was also upregulated in FLS stimulated with IFNγ or IFNγ+PG for 24 hours, but not PG alone (Figure 3B). This confirms that IFNγ, but not PG, is required for immune activation of FLS. When stimulated with IFNγ, FLS also upregulated production of IL-6, CCL2, and TNFα, approximately 2-fold compared to unstimulated controls

and stimulation with *B. burgdorferi* PG alone (Supplemental Figure S1). Interestingly, stimulation with both IFNγ and *B. burgdorferi* PG dampened production of IL-6 in FLS, compared to IFNγ alone, but both stimuli were required for BMDM upregulation of IL-6. Stimulation with *B. burgdorferi* PG alone did not affect the production of CCL2 or TNFα in FLS or BMDM.

MHC-II expression is regulated by the γ-interferon-induced transcriptional coactivator MHC class II transactivator (CIITA) (42). To determine whether IFNγ induces MHC-II expression in FLS in an endogenous, CIITA-dependent manner, FLS were isolated from C57BL/6 mice expressing EGFP under the CIITA promoter (CIITA-GFP reporter mice, a generous gift of Dr. R. Mark Wooten, University of Toledo College of Medicine) and stimulated with IFNγ at concentrations of 0, 0.2, 2, or 20 ng/mL. GFP fluorescence was measured every two hours for four days. FLS from CIITA-GFP reporter mice stimulated with IFNγ at 20 ng/mL had significantly increased fluorescence, particularly after 72-96 hours post-stimulation (consistent with data from Figure 3A), compared to those stimulated with IFNγ at lower concentrations, or compared to background fluorescence of IFNγ-activated FLS isolated from C57BL/6 mice lacking the GFP reporter (Figure 3C).

Murine MHC-II+ FLS activate CD4+ T cells in an antigen-dependent manner

To evaluate whether MHC-II+ FLS can activate CD4+ T cells, we conducted a T cell proliferation assay using activated MHC-II+ FLS co-cultured with CD4+ T cells from OT-II mice, which express a transgenic T cell receptor (TCR) specific for chicken ovalbumin MHC-II antigen $OVA_{323-339}$. Cultured primary C57BL/6 mouse FLS were primed with either IFNγ or IFNγ+PG (as before) for 48 hours to induce MHC-II expression. Following priming, FLS were washed with phosphate buffer saline (PBS) to remove residual IFNγ and PG, placed in fresh media containing antigen (OT-II peptide $OVA_{323-339}$, $OVA_{257-264}$ control peptide, or full-length ovalbumin), and co-cultured with naïve OT-II mouse T cells stained with CFSE proliferation dye

(Figure 4A). Co-culture of OT-II CD4+ T cells with FLS primed with IFNγ and with the OT-II $OVA_{323-339}$ epitope had ~25% increased levels of CD4+ T cell proliferation, compared to ~15% seen using unstimulated FLS (Figure 4B). However, FLS primed with both IFNγ and *B. burgdorferi* PG induced significantly increased (~37%) levels of CD4+ T cell proliferation, compared with the other two conditions (Figure 4B). T cells co-cultured with IFNγ-primed FLS given the $OVA_{257-264}$ control peptide, an alternative MHC-II binding epitope not recognized by the OT-II transgenic TCR, failed to induce T cell proliferation under any conditions (Figure 4B), indicating that T cell proliferation was MHC-II epitope-dependent.

Priming of activated MHC-II+ FLS with PG had a pronounced adjuvant effect on the ability of FLS to induce multiple rounds of T cell proliferation. An average of 30.6% of CD4+ T cells underwent two or more rounds of proliferation when co-cultured with IFNγ+PG-activated MHC-II+ FLS, compared to a significantly lower average of 17.3% of CD4+ T cells that underwent two or more rounds of proliferation when cocultured with IFNγ-activated MHC-II+ FLS without PG (Figure 4B).

Activated MHC-II+ FLS were also able to take up and process extracellular MHC-II antigen. When full-length ovalbumin (10 mM final concentration) was added to the FLS media 24 hours prior to priming with IFNγ +/- PG, activated MHC-II+ FLS induced proliferation of OT-II T cells (Figure 4C), similar to experiments using the OT-II $OVA_{323-339}$ epitope as the MHC-II antigen (Figure 4B).

To characterize the CD4+ T cell responses induced by activated MHC-II+ FLS, we measured cytokines in supernatants collected from FLS-T cell co-culture experiments using the OT-II $OVA_{323-339}$ epitope as antigen (Figure 4D). Supernatants from T cells co-cultured with FLS primed with IFNγ alone had an average of 15.4 pg/mL of IL-10, which was significantly higher than unstimulated FLS (6.4 pg/mL), or FLS primed with IFNγ+PG (6.2 pg/mL). In contrast, supernatants from T cells co-cultured with FLS primed with both IFNγ and PG had elevated

levels of IFNγ (369.5 pg/mL), compared with unprimed FLS (69.2 pg/mL) or FLS primed with IFNγ alone (143.1 pg/mL). As a result, the IFNγ/IL-10 ratio was ~10-fold higher in supernatants from T cells co-cultured with FLS primed with IFNγ+PG, compared with the other two groups, indicating a skew towards a T_H1 effector phenotype. FLS primed with either IFNγ or IFNγ+PG induced production of similarly elevated levels of IL-17A in supernatants of co-culture experiments, compared with unprimed FLS (Figure 4D), suggesting that addition of PG to FLS did not enhance IL-17 production.

DISCUSSION

This study shows that activated MHC-II+ FLS are able to process and present MHC-II antigens, including antigens associated with LA autoimmunity, and can induce CD4+ T cell activation in an antigen-dependent manner, particularly when primed with PG and IFNγ, which partially recapitulates elements of the inflammatory microenvironment within the post-infectious LA synovial lesion. These data also support earlier speculation that MHC-II+ FLS are likely major contributors of HLA-DR-presented peptides derived from ECM proteins that accumulate within the post-infectious LA inflammatory lesion (1, 2, 6). We propose that under pathogenic conditions, localized IFNγ responses during *B. burgdorferi* infection stimulate FLS into an activated MHC-II+ immune effector phenotype. If IFNγ levels within the joint microenvironment become excessive due to autoimmunity and/or accumulation of *B. burgdorferi* PG, activated MHC-II+ FLS can prolong pathogenic T cell reactivity, perpetuating tissue-localized inflammation even in the absence of active infection.

We report that IFNγ induces murine FLS to upregulate numerous genes involved in uptake, processing, and presentation of MHC-II antigen. By utilizing an immunopeptidomics approach, we characterized peptides presented by human LA MHC-II+ FLS and found that these cells are able to present peptides derived from LA autoantigen FN1, which raises the

possibility that these activated MHC-II+ FLS may drive ECM autoimmunity following *B. burgdorferi* infection. We also showed that the adjuvant effects of *B. burgdorferi* PG can fundamentally alter T cell responses induced by MHC-II+ FLS. We show that MHC-II+ FLS, induced by IFNγ, can take up antigen from the environment and induce T cell activation in an antigen-dependent manner, which is exacerbated by *B. burgdorferi* PG to a robust T_H1-like response. Yet, in the absence of PG, T cell proliferation is attenuated and is accompanied by elevated production of the immunomodulatory cytokine IL-10. Overall, these findings support observations in previous studies of post-infectious LA (6, 26, 43), validating our *in vitro* model of LA. Together, these data show that activated MHC-II+ FLS function as inducible APCs to promote ongoing recruitment and activation of IFNγ-producing lymphocytes.

Other studies have demonstrated that excess antigen presentation in the joint is fundamental for driving T cell-mediated autoimmune inflammation against self-peptides derived from proteins at sites of infection associated with synovial tissue damage (1, 21-24). Identification of FN1 as an FLS-presented peptide was particularly noteworthy, since autoreactive CD4+ T cells targeting FN1 and other FLS-derived ECM proteins have a marked T_H1 phenotype, and are detected in over 50% of post-infectious LA patients (1). Our study suggests that retained *B. burgdorferi* PG plays a critical role in perpetuating T_H1 reactivity against autoreactive ECM proteins in post-infectious LA (26).

Our data indicate that activated MHC-II+ FLS phenotypes are plastic, and can be dramatically altered by presence or absence of PG. This finding may have broad implication in other chronic inflammatory joint diseases, particularly when an infection is suspected as an autoimmune trigger. For example, previous reports have identified PG in inflamed synovia from patients with RA (44) and from patients undergoing total knee arthroplasty (28). This study merits a reexamination of the role of PG and other PAMPS in RA autoimmunity. Our study also has potential clinical and therapeutic implications. A recent study showed that part of the

therapeutic effect of JAK inhibitors is reversing the pro-inflammatory effects of activated MHC-II+ FLS by interfering with IFNγ signaling (13).

There are some limitations with our study. While we were able to isolate HLA-DR+ FLS-presented peptides from one patient after *in vitro* stimulation, we are unable to obtain sufficient numbers of FLS directly from patients' tissue to determine what peptides are presented by FLS *ex vivo*. Furthermore, we and others (34) have shown that FLS lack expression of canonical CD80 and CD86 costimulatory molecules. Thus, the source of signal 2 for CD4+ T cell activation is still unknown. As shown in this and other studies, FLS express an altered repertoire of costimulatory molecules such as CD40, ICOS-L, PD-L1, B7-H3 (34, 45), which may provide both pro-inflammatory and anti-inflammatory signals to T cells, depending on the FLS activation state. Further analysis of Signal 2 will be needed to understand the nature of FLS-mediated T cell activation more fully.

In conclusion, this study demonstrates that activated MHC-II+ FLS can present HLA-DR-presented Lyme autoantigens and are inducible APCs that acquire a potent T cell-activating phenotype, particularly when exposed to IFNγ and PG. These findings add to a growing body of evidence that MHC-II+ stromal cells play critical roles in shaping tissue-localized autoimmune CD4+ T cell responses in disease pathogenesis. For example, pancreatic cancer-associated fibroblasts induce activation of autoimmune, pro-tumorigenic regulatory T cell responses in an MHC-II antigen-dependent manner (46). Additionally, IFNγ-activated cardiac fibroblasts are capable of becoming inducible APCs that promote cardiac fibrosis and dysfunction (47). Thus, MHC-II expressing fibroblasts can have profound effects on human health and disease.

ACKNOWLEDGMENTS

We extend our sincerest gratitude to Catherine Costello, PhD, for her invaluable assistance with the immunopeptidomics study. We would also like to acknowledge Mark Wooten, PhD, for

providing the CIITA EGFP-reporter mouse and for reviewing the manuscript; Savannah Neu at the Versiti Flow Cytometry Core for flow cytometry assistance; John Corbett, PhD, Director of the MCW Center for Biomedical Mass Spectrometry Research for providing us with mass spectrometry resources and expertise; and Michael Dwinell, PhD, Director of the MCW Center for Immunology for providing equipment and scientific resources. We would also like to thank Jenifer Coburn, PhD, for generously providing the *B. burgdorferi* strains used in this study.

FUNDING SOURCES

RBL and BLJ were supported by awards from the National Institutes of Health (1R21AI148982-01, 1R01AI173256-01 and 1R01AI178711-01). This work was supported by The Assistant Secretary of Defense for Health Affairs through the Tick-Borne Disease Research Program, endorsed by the Department of Defense under Award No. W81XWH-22-1- 0728. Opinions, interpretations, conclusions and recommendations are those of the author and are not necessarily endorsed by the Department of Defense.

MATERIALS AND METHODS

Ethics statement

Mice were housed in the Medical College of Wisconsin Biomedical Resource Center (Milwaukee, WI), following strict adherence to the guidelines according to the National Institutes of Health for the care and use of laboratory animals, as described in the Guide for the Care and Use of Laboratory Animals, 8th Edition. Protocols conducted in this study were approved and carried out in accordance with the Medical College of Wisconsin Institutional Animal Care and Use Committee (IACUC protocol number AUA00006528). Mouse experiments were performed under isoflurane anesthesia, and every effort was made to minimize suffering.

The study “Immunity in Lyme Arthritis” was approved by the Human Investigations Committee at Massachusetts General Hospital (MGH), according to principles for medical

research involving human subjects expressed in the World Medical Association Declaration of Helsinki. Written informed consent was obtained from all participants 18 years of age or older, or from patient and a parent or guardian of those between the ages of 12 and 17.

Patients

All patients with Lyme disease met the Centers for Disease Control and Prevention criteria for *B. burgdorferi* infection (48). All patients had swollen knees and high IgG antibody responses to *B. burgdorferi,* as determined by ELISA and Western blot. LA patients received treatment according to an algorithm (17), as mentioned in the guidelines of the Infectious Diseases Society of America (49).

Human LA FLS stimulation and RNA purification

Human LA FLS gene expression data were generated as part of an earlier study (6). Briefly, FLS ($2x10^5$ cells/well) from 5 patients were each stimulated with a *B. burgdorferi* RST1 OspC type A strain at a multiplicity of infection (MOI) of 25 bacteria per cell, IFNγ (10 ng/mL), or both *B. burgdorferi* + IFNγ for 16 hours, or left unstimulated. Culture supernatants were collected and stored at -80° C for cytokine analysis. Cells were washed three times in ice-cold PBS. Approximately 100 ng of total RNA was recovered from stimulated FLS using an RNeasy kit (Qiagen). NEB Next Poly(A) Ultra Directional processing kit (New England Biolabs) was used to separate mRNA from rRNA. FLS RNA quality was determined using a Bioanalyzer (Agilent), and low-quality RNA samples were excluded from this study. RNA libraries were constructed using the NEBNext Ultra RNA Prep Kit for Illumina (New England Biolabs). Libraries were sequenced to a depth of ~25 million paired-end, 100 base-pair reads (Hi-Seq PE100 Reagent Kit, Illumina). Library preparation, sequencing, and bioinformatics were performed by the MGH NextGen Sequencing and Bioinformatics Core Facilities.

Immunofluorescence microscopy

Biopsies from four patients with post-infectious LA, which had been previously collected at the time of surgery, were immediately flash-frozen in optimal cutting temperature (OCT) medium and stored in liquid nitrogen. Two sections from each biopsy were stained with Vimentin-Alexa Fluor 647 and HLA-DR-Alexa Fluor 488 (BioLegend). Imaging was performed using a Zeiss LSM 780 confocal microscope. Semi-quantitative analysis of HLA-DR and vimentin staining was conducted for each biopsy. Intensity was calculated in three 20X frames from each sample using Zen Black software (Zeiss).

Immunoaffinity purification of MHC-II peptide complexes

Human synovial FLS from patients with LA were cultured *in vitro* in complete Dulbecco's modified eagle's medium (DMEM) supplemented with 20% fetal bovine serum (FBS), 1% L-glutamine, 1% nonessential amino acids and 5 ng/mL of recombinant human FGF-basic (BioLegend #792504). Cells were stimulated with *B. bugdorferi* (B31-A3 strain; MOI of 10) for 65 hours and 10 ng/mL of recombinant human IFNγ (BioLegend 713906) for 48 hours. MHC-II molecules were isolated by immunoaffinity capture and MHC-bound peptides were identified by LC-MS/MS using Thermo Orbitrap Fusion Lumos technology.

The procedures used for MHC II peptide isolation were similar to those published by Seward, et al. (50). Water (Fisher Scientific) was HPLC grade. CNBr-activated Sepharose beads (GE Healthcare) were used for coupling of the I-A/I-E-specific antibody (M5/114.15.2; 4 mg). Before antibody coupling, the Sepharose beads were pre-hydrolyzed in coupling buffer (0.1M $NaHCO_3$, 0.5M NaCl, pH 8.5) to reduce the number of reactive groups on the beads. After pre-hydrolysis, the antibody was incubated with the beads for 1 h followed by a 3 h incubation with blocking buffer (0.015 g/mL glycine in coupling buffer). Uncoupled beads were prepared identically but without antibody. Cell lysates were incubated with uncoupled beads for 4 hours at

4°C and then with M5/114.15.2-conjugated beads overnight at 4°C. Beads were washed 4 × 15 min and 1 × 30 min with 14 mL of 1% CHAPS-containing lysis buffer and then 4 × 15 min and 1 × 40 min with 14 mL of High NaCl wash buffer (150 mM NaCl, 20 mM Tris-HCl, pH 8). Beads were transferred to a column (5 mL, Pierce) and washed with 50 mL of High NaCl wash buffer followed by 50 mL of No NaCl wash buffer (20 mM Tris-HCl, pH 8) by gravity flow. Residual buffer was removed by centrifugation for 2 min at 800 × g. Peptides were eluted by 7 × 5 min incubations at RT with 0.7 mL of 0.5% formic acid followed by centrifugation for 2 min at 800 × g to collect eluates.

LC-MS/MS

Peptide extracts were dried and re-dissolved in 28 µL of 2% acetonitrile/0.1% formic acid with vortexing and sonication. After centrifugation, 24 µL of the supernatants were transferred to autosampler vials for duplicate injections of 10 µL onto a 75 µm x 50 cm C_{18} column (Thermo Acclaim PepMap 100 C_{18}). The peptides were separated and subsequently analyzed on a Thermo Orbitrap Fusion Lumo MS via two technical replicate injections using a data-dependent acquisition (DDA) HCD MS2 instrument method.

Protein and peptide database searching

MS data were analyzed using Proteome Discoverer 2.4 (Thermo) platform. SequestHT was used as a search algorithm. Fixed Value (FV) and Target-Decory (TD) peptide-spectrum match (PSM) validators and Protein FDR validator were used to identify potential PSM-peptide matches. For FV validation, PSMs with cross-correlation scores (Xcorr) lower than 2.5 were excluded as potential matches. Proteome databases searched for this study were *Borrelia burgdorferi* (N40 and B31), Human (Swissprot, with isoforms), and MaxQuant contaminants. Oxidation (M), acetylation (protein N-terminus), deamidation (N, Q), and Gln->pyro-Glu dynamic modifications were allowed. Target FDR for PSMs and peptides were 0.01 (strict) or 0.05

(relaxed). Immune Epitope Database (IEDB) (http://tools.iedb.org/mhcii) was used to identify other predicted T cell epitopes of interest. Predicted peptide binding grooves were determined using NetMHCIIpan-4.0, DTU Health Tech (services.healthtech.dtu.dk/services/NetMHCIIpan-4.0/). KEGG, WIKI, and Gene Ontology analyses were performed on identified peptides using the Gene Functional Classification Tool by DAVID Bioinformatics Resources, NIAID/NIH.

Bacteria and mouse strains

Mouse strains C57B6/J (B6) and B6.Cg-Tg(TcraTcrb)425Cbn/J (OT-II) were acquired from Jackson Laboratory. The class II major histocompatibility complex trans-activator (CIITA) EGFP-reporter mouse was generously provided by Dr. R. Mark Wooten and was generated as described (51). Briefly, a 129/Sv mouse strain carrying an EGFP label on all MHC β-chains was generated and back-crossed onto the C57BL/6J background for 7 generations. For the *in vitro* stimulation experiments using live bacteria, we used *B. burgdorferi* strain B31-A2 generously provided by Dr. Jenifer Coburn.

Primary cell stimulation and flow cytometry analysis

Bone marrow-derived macrophages (BMDM) were obtained by culturing adherent bone marrow cells from C57BL6/J (B6) mice with 10 ng/mL M-CSF (BioLegend #576304) for 5 days. Primary murine FLS were isolated from B6 hind leg ankle joints as described (41), passaged 3 times to obtain purified FLS, and stored in liquid nitrogen. Primary human FLS were collected, isolated, and passaged as described (6). HLA-typing was performed in the Red Cross Laboratory in Dedham, Massachusetts. Both murine and human FLS were used at passage ≤ four for each experiment and FLS purity was determined by flow cytometric analysis (CD90+, CD45-, CD11b-). Cells were plated in each well of a 24-well polystyrene plate at $1x10^5$ cells/mL in complete Dulbecco's modified eagle's medium (DMEM) supplemented with 10% fetal bovine serum (FBS), 2 mM L-glutamine, 100 U/mL penicillin, 100 µg/mL streptomycin, and 1%

nonessential amino acids. Cells were stimulated for 48 hours with IFNγ (20 ng/ mL), *B. burgdorferi* (N40) (1x106 cells/ mL), PG muropeptides (Sigma #77140) or *B. burgdorferi* PG (10 µg/ mL). *B. burgdorferi* PG was purified as previously described (52). After PG purification, intact sacculi were digested with mutanolysin (Sigma) and the purity was confirmed by liquid chromatography-mass spectrometry using methods published elsewhere (53). FLS and BMDMs were collected and washed with phosphate buffer saline (PBS) before incubation with cell surface antibodies for 20 minutes. FLS and BMDMs were incubated with fluorochrome-coupled antibodies at the manufacturers' recommended concentrations against CD11b (Biolegend #101228), I-ab (BioLegend #116418), CD90.2 (Biolegend #140324), and CD54 (Biolegend #116141). Cells were analyzed using FACS Celesta (Beckman Coulter) and FlowJo v.10.7.1 software.

Incucyte™ imaging of CIITA EGFP-reporter FLS

CIITA EGFP-reporter FLS (passage four), were stimulated with 0, 0.2, 2, or 20 ng/mL IFNγ and compared to non-GFP-tagged controls. Cells were plated at 70,000 cells per well in 100 µl of medium in a 96-well plate and were allowed to rest overnight in a 32°C incubator with 5% CO_2. Green fluorescence (ex:440-480 nm, em:504-544 nm) was used to detect the EGFP reporter and analyzed by IncuCyte imaging with images taken every two hours for 96 hours total at 10X objective. Statistical analysis was performed using Tukey's multiple comparisons test ($p<0.05$). Error bars represent standard deviation.

Cytokine analysis

Cell-free supernatants were collected and cytokine secretion was assayed by LegendPlex (BioLegend #740446) multiplex analysis according to the manufacturers' instructions using the Celesta Flow cytometer (Beckman Coulter) and analyzed with

LegendPlex online software. Cytokine analysis was performed using the LEGENDplex Mouse Inflammation Panel (Biolegend 740446) to quantify 13 inflammatory cytokines/chemokines (IL-1β, IL-1α, IFN-γ, TNF-α, MCP-1 (CCL2), IL-6, IL-27, IL-10, IL-12p70, IL-17A, IFNβ, IL-23, and GM-CSF).

T cell proliferation assay and flow cytometric analysis

Primary synovial FLS were passaged approximately five times prior to co-culture, as FLS recovered directly from frozen stock (stored in liquid nitrogen at passage three) exhibited dampened responses to inflammatory stimuli (data not shown). FLS cultured at a concentration of $1x10^5$ cells/ well were seeded in flat-bottom 24-well tissue culture plates and stimulated for 48 hours with IFNγ, *B. burgdorferi* PG, or both simultaneously in DMEM with 2% FBS at 37ºC. Care was taken to not disturb cultured cells and any samples with non-adherent FLS were excluded. CD3+ T cells were isolated from spleens of 6-to-8-week-old OT-II mice by MojoSort mouse CD3+ T cell isolation kit (Biolegend 480024). APCs were washed with PBS and co-cultured with CD3+ T cells at a concentration of approximately $5x10^5$-$10x10^5$ cells/ mL in complete RPMI medium (10% FBS, 2 mM L-glutamine, 50 µM β-mercaptoethanol, 100 U/mL penicillin, 100 µg/mL streptomycin, 1% nonessential amino acids, 1% HEPES, 1% sodium pyruvate) for 5 days. Samples were supplemented with either the cognate $OVA_{323-339}$ peptide or an alternative non-reactive $OVA_{257-264}$ peptide at 2 ug/mL, as well as IL-2 (0.5 ug/mL) to maintain T cell viability. T cells were collected and washed with PBS before incubation with cell surface antibodies for 20 minutes. CD3+ T cells were stained with fluorochrome-coupled antibodies at the manufacturers' recommended concentrations against CD3 (BioLegend #100216), CD4 (BioLegend #100412), and CD8 (BioLegend #100725). Cells were analyzed using FACS Celesta (Beckman Coulter) and FlowJo v.10.7.1 software. Cell-free supernatants were collected, and cytokine secretion was assayed by LegendPlex (BioLegend #740446) multiplex

analysis and according to the manufacturers' instructions using the Celesta Flow cytometer (Beckman Coulter) and analyzed with LegendPlex online software.

Statistical analysis

Statistically significant differences in surface marker expression and cytokine secretion levels between stimulated versus unstimulated cellular groups were determined by one-way ANOVA and Tukey's multiple comparisons. All statistical analyses were performed using GraphPad Prism (v.9). For gene expression analysis, copies per million reads (CPMR) was used to normalize gene expression.

FIGURES AND FIGURE LEGENDS

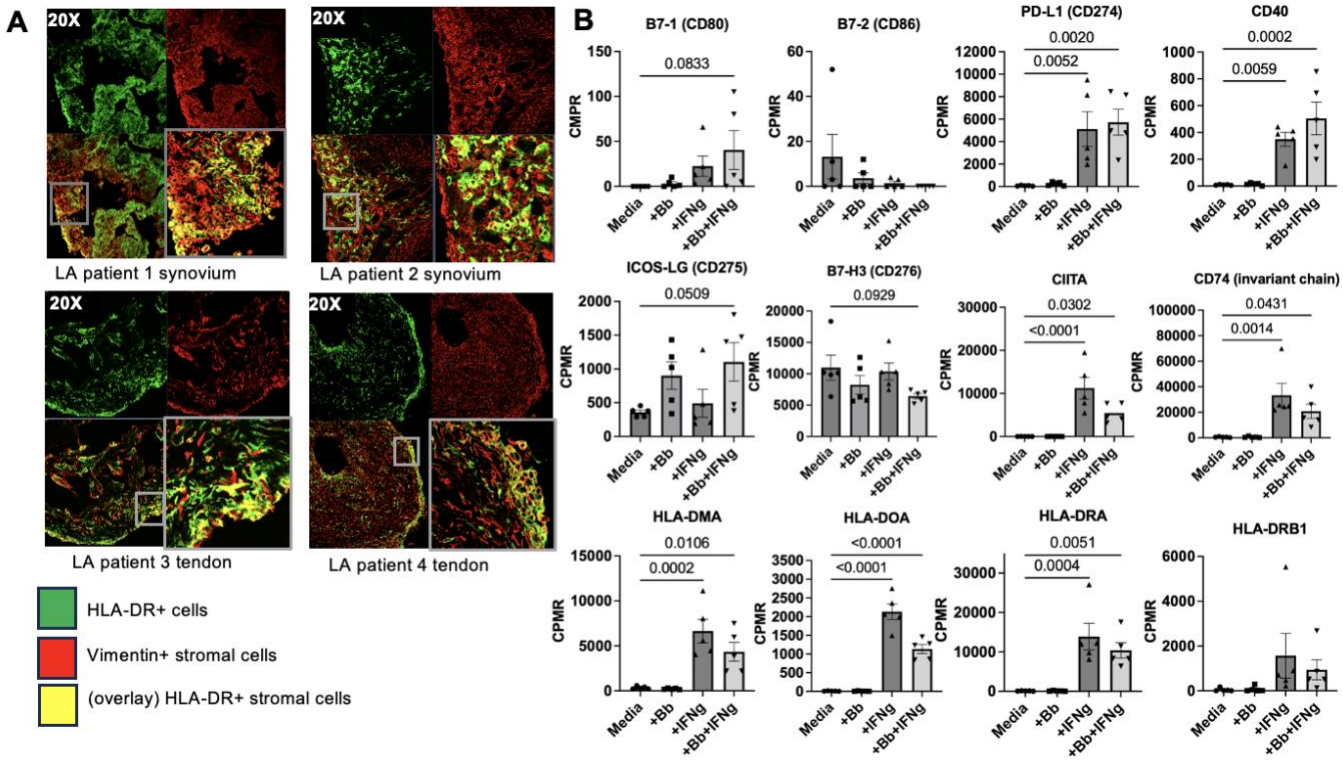

Figure 1. FLS expression of MHC class II and costimulatory molecules is induced by IFNγ

Characterization of synovial and tendon tissue samples from four different LA patients. Representative images of co-localization of HLA-DR and vimentin in two LA synovial and two tendon tissue biopsies (A). Bulk RNA sequencing analysis of one LA patient's (Patient 1) FLS stimulated *ex vivo* with IFNɣ, *Borrelia burgdorferi (Bb)*, or both (B). Statistical analysis was performed using Tukey's multiple comparisons test (p values indicated in figure). Error bars represent standard errors from mean. CPMR: copies per million reads.

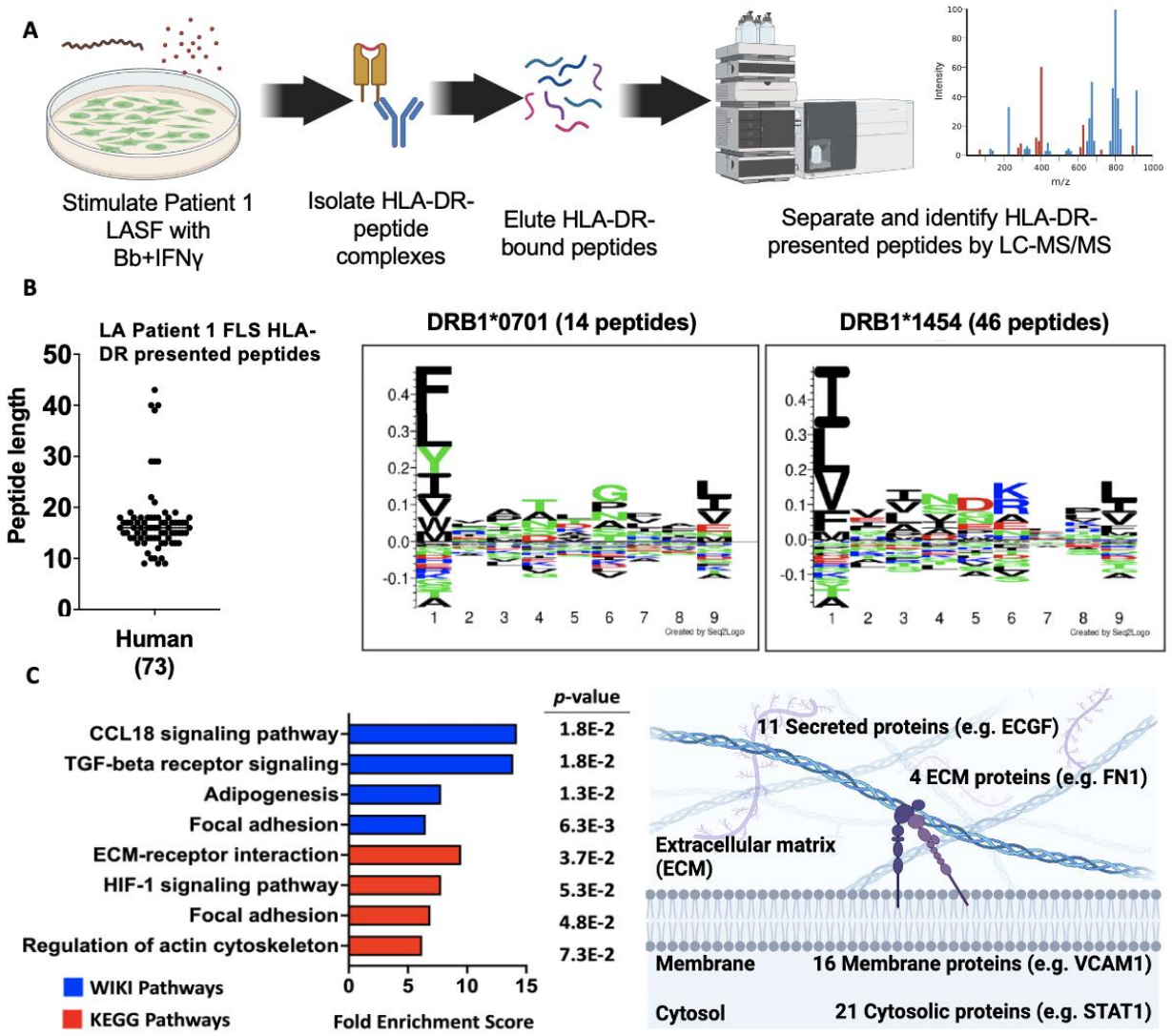

Figure 2. Human LA FLS present MHC-II peptides derived from Lyme autoantigens Immunopeptidomics screen of unique LA patient FLS HLA-DR presented peptides (A). Peptide length and predicted HLA binding motifs of peptides predicted by both Fixed Value (FV) and Target Decoy (TD) analyses corresponding with LA patient 1 HLA-DR type (B). WIKI Pathways, KEGG Pathways, and Gene Ontology cellular localization analyses showing enriched pathways and cellular localization associated with source proteins (C).

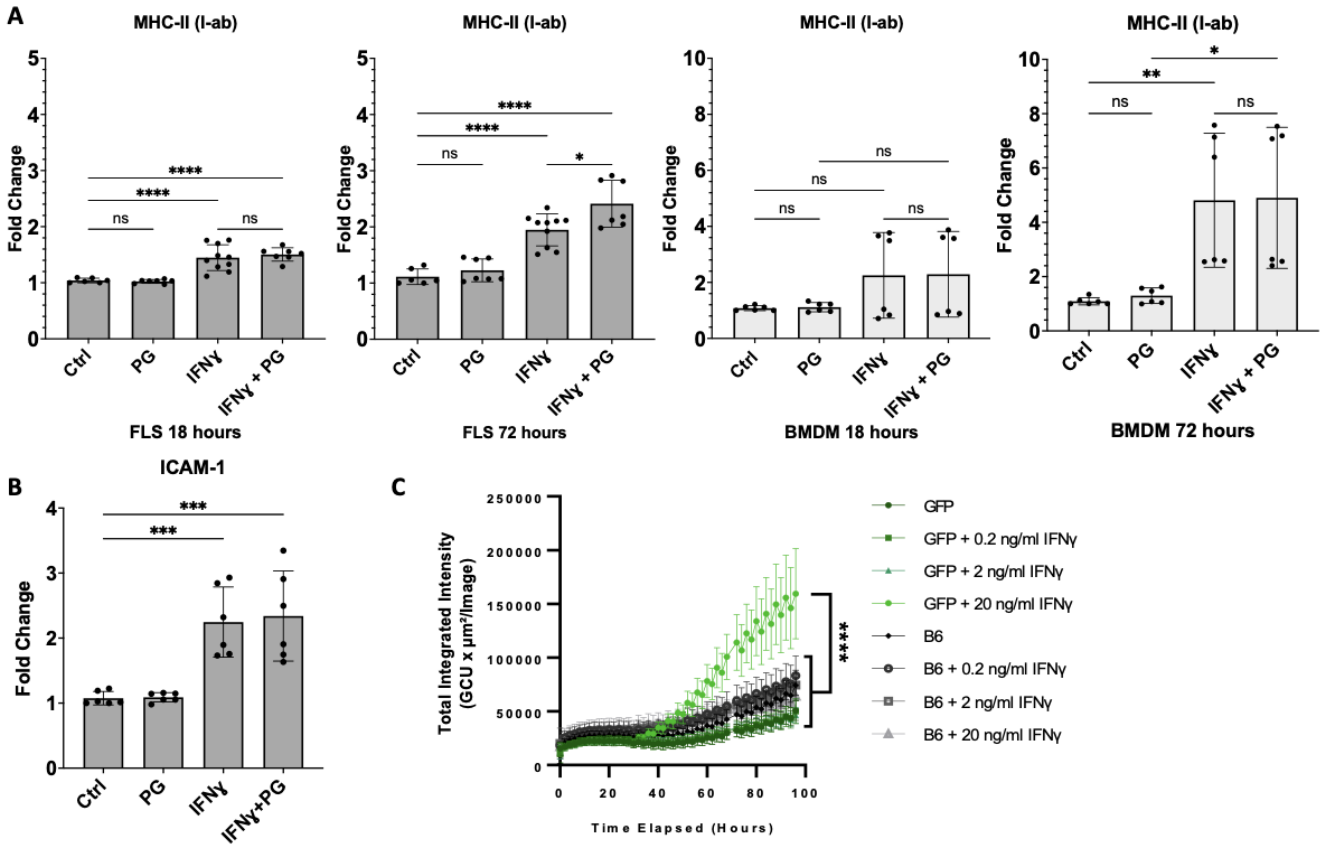

Figure 3. Murine FLS upregulate MHC-II in response to IFNɣ

Surface expression of MHC-II by primary B6 murine FLS or BMDMs stimulated with *B. burgdorferi* PG (10 µg/ml), IFNɣ (20 ng/ ml), or both for 18 or 72 hours (A). A separate experiment demonstrating expression of ICAM by FLS in response to IFNɣ and *B. burgdorferi* PG stimulation for 24 hours (B). Data pooled from two independent experiments with three technical replicates (A-B). CIITA EGFP-reporter mouse FLS (passage 4) were stimulated with 0, 0.2, 2, or 20 ng/mL IFNɣ and compared to non-EGFP expressing control B6 FLS. Fluorescence was analyzed by IncuCyte imaging with images taken every 2 hours for 96 hours total at 10X objective (C). All statistical analysis performed using Tukey's multiple comparisons test ($p<0.05$). Error bars represent standard deviation.

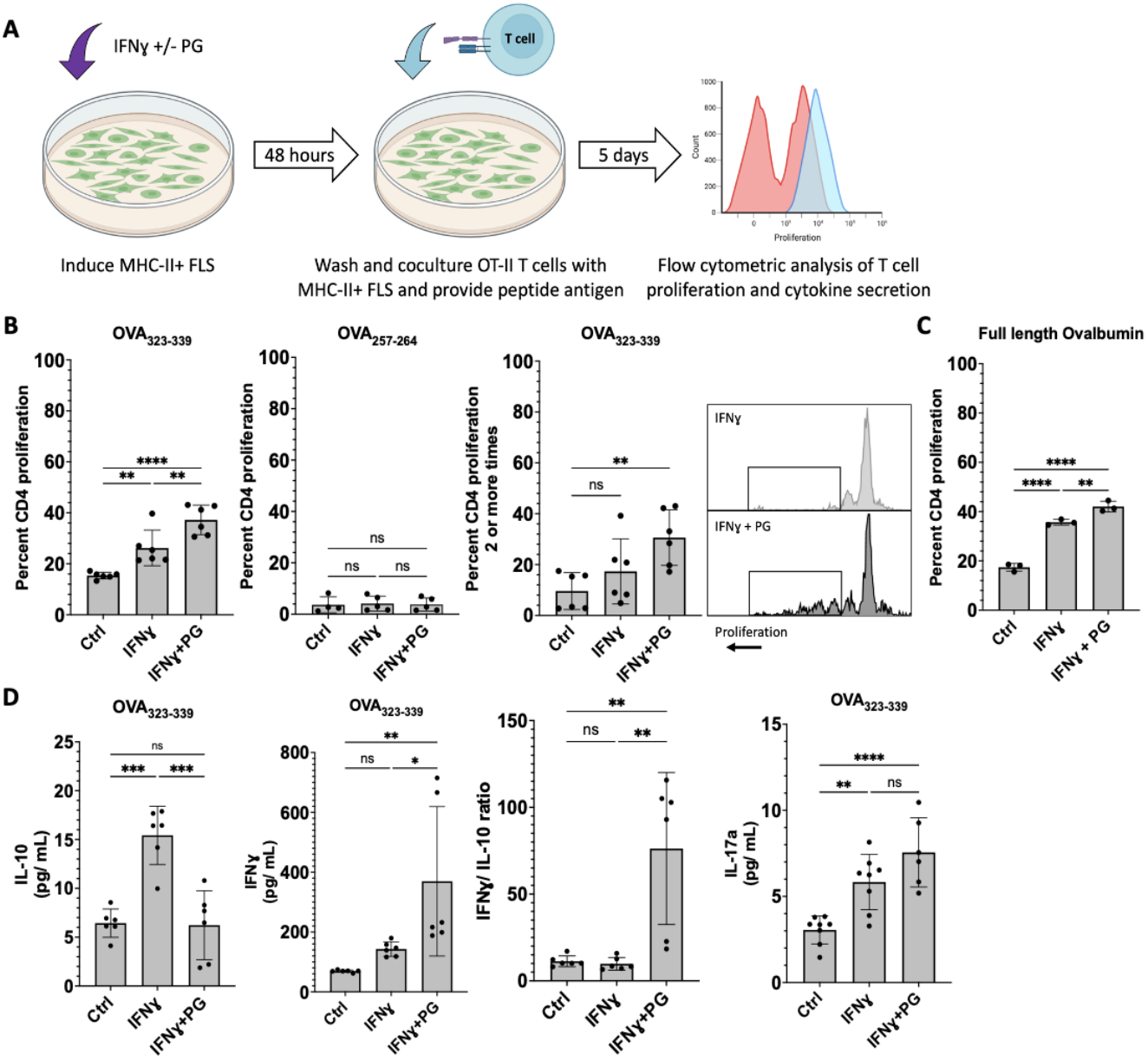

Figure 4. Murine activated MHC-II+ FLS induce CD4+ T cell activation in an antigen-dependent manner

MHC-II+ FLS were induced with either IFNɣ alone or IFNɣ and *B. burgdorferi* PG for 48 hours and washed prior to isolation and coculture of OT-II mouse T cells for 5 days and subsequent analysis by flow cytometry (A). Percentage of proliferating CD4+ T cells and cells that completed two or more rounds of replication, induced by MHC-II+ FLS when loaded with ovalbumin peptides (B). Percentage of proliferating CD4+ T cells induced by MHC-II+ FLS when

loaded with full-length ovalbumin (C). Co-culture cytokine analysis of IFNɣ, IL-10, and IL-17a production (D). All data were pooled from two independent experiments with three technical replicates and statistical analysis was performed using Tukey's multiple comparisons test ($p<0.05$). Error bars represent standard deviation.

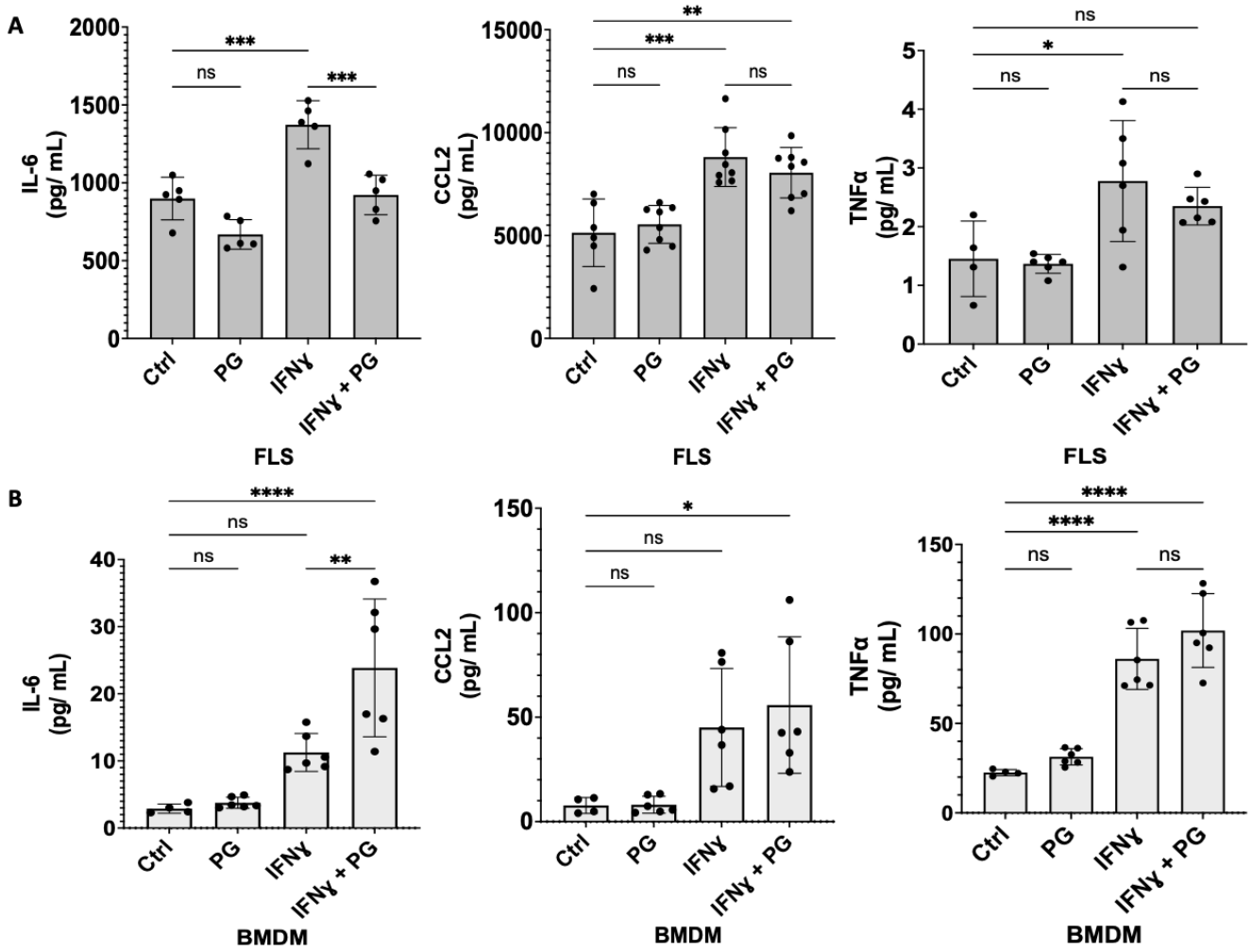

Supplemental Figure S1. Murine MHC-II+ FLS upregulate proinflammatory mediators in response to IFNɣ

Production of IL-6, TNFα, and CCL2 by primary B6 murine FLS (A) and BMDM (B) stimulated with *B. burgdorferi* PG (10 µg/ml), IFNɣ (20 ng/ ml), or both for ~24 hrs. All data pooled from two

independent experiments and statistical analysis was performed using Tukey's multiple comparisons test ($p<0.05$). Error bars represent standard deviation.

References

1. Kanjana K, Strle K, Lochhead RB, Pianta A, Mateyka LM, Wang Q, et al. Autoimmunity to synovial extracellular matrix proteins in patients with post-infectious lyme arthritis. J Clin Invest. 2023.
2. Lochhead RB, Strle K, Arvikar SL, Weis JJ, Steere AC. Lyme arthritis: linking infection, inflammation and autoimmunity. Nat Rev Rheumatol. 2021;17(8):449-61.
3. Nygaard G, Firestein GS. Restoring synovial homeostasis in rheumatoid arthritis by targeting fibroblast-like synoviocytes. Nat Rev Rheumatol. 2020;16(6):316-33.
4. Smith MH, Gao VR, Periyakoil PK, Kochen A, DiCarlo EF, Goodman SM, et al. Drivers of heterogeneity in synovial fibroblasts in rheumatoid arthritis. Nat Immunol. 2023;24(7):1200-10.
5. Wei K, Nguyen HN, Brenner MB. Fibroblast pathology in inflammatory diseases. J Clin Invest. 2021;131(20).
6. Lochhead RB, Ordonez D, Arvikar SL, Aversa JM, Oh LS, Heyworth B, et al. Interferon-gamma production in Lyme arthritis synovial tissue promotes differentiation of fibroblast-like synoviocytes into immune effector cells. Cell Microbiol. 2019;21(2):e12992.
7. Plikus MV, Wang X, Sinha S, Forte E, Thompson SM, Herzog EL, et al. Fibroblasts: Origins, definitions, and functions in health and disease. Cell. 2021;184(15):3852-72.
8. Carmona-Rivera C, Carlucci PM, Moore E, Lingampalli N, Uchtenhagen H, James E, et al. Synovial fibroblast-neutrophil interactions promote pathogenic adaptive immunity in rheumatoid arthritis. Sci Immunol. 2017;2(10).
9. Croft AP, Campos J, Jansen K, Turner JD, Marshall J, Attar M, et al. Distinct fibroblast subsets drive inflammation and damage in arthritis. Nature. 2019;570(7760):246-51.
10. Mizoguchi F, Slowikowski K, Wei K, Marshall JL, Rao DA, Chang SK, et al. Functionally distinct disease-associated fibroblast subsets in rheumatoid arthritis. Nat Commun. 2018;9(1):789.
11. Tran CN, Davis MJ, Tesmer LA, Endres JL, Motyl CD, Smuda C, et al. Presentation of arthritogenic peptide to antigen-specific T cells by fibroblast-like synoviocytes. Arthritis Rheum. 2007;56(5):1497-506.
12. Zhang F, Wei K, Slowikowski K, Fonseka CY, Rao DA, Kelly S, et al. Defining inflammatory cell states in rheumatoid arthritis joint synovial tissues by integrating single-cell transcriptomics and mass cytometry. Nat Immunol. 2019;20(7):928-42.
13. Zhao S, Grieshaber-Bouyer R, Rao DA, Kolb P, Chen H, Andreeva I, et al. Effect of JAK Inhibition on the Induction of Proinflammatory HLA-DR+CD90+ Rheumatoid Arthritis Synovial Fibroblasts by Interferon-gamma. Arthritis Rheumatol. 2022;74(3):441-52.
14. Alivernini S, MacDonald L, Elmesmari A, Finlay S, Tolusso B, Gigante MR, et al. Distinct synovial tissue macrophage subsets regulate inflammation and remission in rheumatoid arthritis. Nat Med. 2020;26(8):1295-306.
15. Dong Y, Zhou G, Cao W, Xu X, Zhang Y, Ji Z, et al. Global seroprevalence and sociodemographic characteristics of Borrelia burgdorferi sensu lato in human populations: a systematic review and meta-analysis. BMJ Glob Health. 2022;7(6).

652 16. Kugeler KJ, Schwartz AM, Delorey MJ, Mead PS, Hinckley AF. Estimating the Frequency
653 of Lyme Disease Diagnoses, United States, 2010-2018. Emerg Infect Dis. 2021;27(2):616-9.
654 17. Arvikar SL, Steere AC. Lyme Arthritis. Infect Dis Clin North Am. 2022;36(3):563-77.
655 18. Snydman DR, Schenkein DP, Berardi VP, Lastavica CC, Pariser KM. Borrelia burgdorferi in
656 joint fluid in chronic Lyme arthritis. Ann Intern Med. 1986;104(6):798-800.
657 19. Steere AC. Lyme disease. N Engl J Med. 1989;321(9):586-96.
658 20. Steere AC, Schoen RT, Taylor E. The clinical evolution of Lyme arthritis. Ann Intern Med.
659 1987;107(5):725-31.
660 21. Crowley JT, Drouin EE, Pianta A, Strle K, Wang Q, Costello CE, et al. A Highly Expressed
661 Human Protein, Apolipoprotein B-100, Serves as an Autoantigen in a Subgroup of Patients With
662 Lyme Disease. J Infect Dis. 2015;212(11):1841-50.
663 22. Crowley JT, Strle K, Drouin EE, Pianta A, Arvikar SL, Wang Q, et al. Matrix
664 metalloproteinase-10 is a target of T and B cell responses that correlate with synovial pathology
665 in patients with antibiotic-refractory Lyme arthritis. J Autoimmun. 2016;69:24-37.
666 23. Drouin EE, Seward RJ, Strle K, McHugh G, Katchar K, Londono D, et al. A novel human
667 autoantigen, endothelial cell growth factor, is a target of T and B cell responses in patients with
668 Lyme disease. Arthritis Rheum. 2013;65(1):186-96.
669 24. Pianta A, Drouin EE, Crowley JT, Arvikar S, Strle K, Costello CE, et al. Annexin A2 is a
670 target of autoimmune T and B cell responses associated with synovial fibroblast proliferation in
671 patients with antibiotic-refractory Lyme arthritis. Clin Immunol. 2015;160(2):336-41.
672 25. Bockenstedt LK, Gonzalez DG, Haberman AM, Belperron AA. Spirochete antigens persist
673 near cartilage after murine Lyme borreliosis therapy. J Clin Invest. 2012;122(7):2652-60.
674 26. Jutras BL, Lochhead RB, Kloos ZA, Biboy J, Strle K, Booth CJ, et al. Borrelia burgdorferi
675 peptidoglycan is a persistent antigen in patients with Lyme arthritis. Proc Natl Acad Sci U S A.
676 2019;116(27):13498-507.
677 27. Schrijver IA, Melief MJ, Markusse HM, Van Aelst I, Opdenakker G, Hazenberg MP, et al.
678 Peptidoglycan from sterile human spleen induces T-cell proliferation and inflammatory
679 mediators in rheumatoid arthritis patients and healthy subjects. Rheumatology (Oxford).
680 2001;40(4):438-46.
681 28. Holub MN, Wahhab A, Rouse JR, Danner R, McClune MM, Dressler JM, et al.
682 Peptidoglycan in osteoarthritis synovial tissue is associated with joint inflammation. Res Sq.
683 2023.
684 29. Chiu YC, Lin CY, Chen CP, Huang KC, Tong KM, Tzeng CY, et al. Peptidoglycan enhances
685 IL-6 production in human synovial fibroblasts via TLR2 receptor, focal adhesion kinase, Akt, and
686 AP-1- dependent pathway. J Immunol. 2009;183(4):2785-92.
687 30. Kyburz D, Rethage J, Seibl R, Lauener R, Gay RE, Carson DA, et al. Bacterial
688 peptidoglycans but not CpG oligodeoxynucleotides activate synovial fibroblasts by toll-like
689 receptor signaling. Arthritis Rheum. 2003;48(3):642-50.
690 31. Haupl T, Hahn G, Rittig M, Krause A, Schoerner C, Schonherr U, et al. Persistence of
691 Borrelia burgdorferi in ligamentous tissue from a patient with chronic Lyme borreliosis. Arthritis
692 Rheum. 1993;36(11):1621-6.
693 32. Steere AC. Musculoskeletal manifestations of Lyme disease. Am J Med.
694 1995;98(4A):44S-8S; discussion 8S-51S.

695 33. Miller JB, Albayda J, Aucott JN. The Value of Musculoskeletal Ultrasound for Evaluation
696 of Postinfectious Lyme Arthritis. J Clin Rheumatol. 2022;28(2):e605-e8.
697 34. Tran CN, Thacker SG, Louie DM, Oliver J, White PT, Endres JL, et al. Interactions of T cells
698 with fibroblast-like synoviocytes: role of the B7 family costimulatory ligand B7-H3. J Immunol.
699 2008;180(5):2989-98.
700 35. Wang Q, Drouin EE, Yao C, Zhang J, Huang Y, Leon DR, et al. Immunogenic HLA-DR-
701 Presented Self-Peptides Identified Directly from Clinical Samples of Synovial Tissue, Synovial
702 Fluid, or Peripheral Blood in Patients with Rheumatoid Arthritis or Lyme Arthritis. J Proteome
703 Res. 2017;16(1):122-36.
704 36. Coleman JL, Crowley JT, Toledo AM, Benach JL. The HtrA protease of Borrelia
705 burgdorferi degrades outer membrane protein BmpD and chemotaxis phosphatase CheX. Mol
706 Microbiol. 2013;88(3):619-33.
707 37. Barbour AG, Jasinskas A, Kayala MA, Davies DH, Steere AC, Baldi P, et al. A genome-wide
708 proteome array reveals a limited set of immunogens in natural infections of humans and white-
709 footed mice with Borrelia burgdorferi. Infect Immun. 2008;76(8):3374-89.
710 38. Pishesha N, Harmand TJ, Ploegh HL. A guide to antigen processing and presentation. Nat
711 Rev Immunol. 2022;22(12):751-64.
712 39. Schraufstatter IU, Zhao M, Khaldoyanidi SK, Discipio RG. The chemokine CCL18 causes
713 maturation of cultured monocytes to macrophages in the M2 spectrum. Immunology.
714 2012;135(4):287-98.
715 40. Helble JD, McCarthy JE, Sawden M, Starnbach MN, Hu LT. The PD-1/PD-L1 pathway is
716 induced during Borrelia burgdorferi infection and inhibits T cell joint infiltration without
717 compromising bacterial clearance. PLoS Pathog. 2022;18(10):e1010903.
718 41. Lochhead RB, Sonderegger FL, Ma Y, Brewster JE, Cornwall D, Maylor-Hagen H, et al.
719 Endothelial cells and fibroblasts amplify the arthritogenic type I IFN response in murine Lyme
720 disease and are major sources of chemokines in Borrelia burgdorferi-infected joint tissue. J
721 Immunol. 2012;189(5):2488-501.
722 42. Mach B, Steimle V, Martinez-Soria E, Reith W. Regulation of MHC class II genes: lessons
723 from a disease. Annu Rev Immunol. 1996;14:301-31.
724 43. Lochhead RB, Arvikar SL, Aversa JM, Sadreyev RI, Strle K, Steere AC. Robust interferon
725 signature and suppressed tissue repair gene expression in synovial tissue from patients with
726 postinfectious, Borrelia burgdorferi-induced Lyme arthritis. Cell Microbiol. 2019;21(2):e12954.
727 44. van der Heijden IM, Wilbrink B, Tchetverikov I, Schrijver IA, Schouls LM, Hazenberg MP,
728 et al. Presence of bacterial DNA and bacterial peptidoglycans in joints of patients with
729 rheumatoid arthritis and other arthritides. Arthritis Rheum. 2000;43(3):593-8.
730 45. Sempowski GD, Chess PR, Phipps RP. CD40 is a functional activation antigen and B7-
731 independent T cell costimulatory molecule on normal human lung fibroblasts. J Immunol.
732 1997;158(10):4670-7.
733 46. Huang H, Wang Z, Zhang Y, Pradhan RN, Ganguly D, Chandra R, et al. Mesothelial cell-
734 derived antigen-presenting cancer-associated fibroblasts induce expansion of regulatory T cells
735 in pancreatic cancer. Cancer Cell. 2022;40(6):656-73 e7.
736 47. Ngwenyama N, Kaur K, Bugg D, Theall B, Aronovitz M, Berland R, et al. Antigen
737 presentation by cardiac fibroblasts promotes cardiac dysfunction. Nat Cardiovasc Res.
738 2022;1(8):761-74.

739 48. Centers for Disease C, Prevention. Recommendations for test performance and
740 interpretation from the Second National Conference on Serologic Diagnosis of Lyme Disease.
741 MMWR Morb Mortal Wkly Rep. 1995;44(31):590-1.
742 49. Lantos PM, Rumbaugh J, Bockenstedt LK, Falck-Ytter YT, Aguero-Rosenfeld ME,
743 Auwaerter PG, et al. Clinical Practice Guidelines by the Infectious Diseases Society of America
744 (IDSA), American Academy of Neurology (AAN), and American College of Rheumatology (ACR):
745 2020 Guidelines for the Prevention, Diagnosis and Treatment of Lyme Disease. Clin Infect Dis.
746 2021;72(1):1-8.
747 50. Seward RJ, Drouin EE, Steere AC, Costello CE. Peptides presented by HLA-DR molecules
748 in synovia of patients with rheumatoid arthritis or antibiotic-refractory Lyme arthritis. Mol Cell
749 Proteomics. 2011;10(3):M110 002477.
750 51. Boes M, Cerny J, Massol R, Op den Brouw M, Kirchhausen T, Chen J, et al. T-cell
751 engagement of dendritic cells rapidly rearranges MHC class II transport. Nature.
752 2002;418(6901):983-8.
753 52. Davis MM, Brock AM, DeHart TG, Boribong BP, Lee K, McClune ME, et al. The
754 peptidoglycan-associated protein NapA plays an important role in the envelope integrity and in
755 the pathogenesis of the lyme disease spirochete. PLoS Pathog. 2021;17(5):e1009546.
756 53. DeHart TG, Kushelman MR, Hildreth SB, Helm RF, Jutras BL. The unusual cell wall of the
757 Lyme disease spirochaete Borrelia burgdorferi is shaped by a tick sugar. Nat Microbiol.
758 2021;6(12):1583-92.
759